



Multi-objective process route optimization considering carbon emissions

Guang-hui Zhou^{1,2} · Chang-le Tian¹ · Jun-jie Zhang¹ · Feng-tian Chang¹ · Qi Lu¹

Received: 15 October 2017 / Accepted: 15 January 2018 / Published online: 8 February 2018
© Springer-Verlag London Ltd., part of Springer Nature 2018

Abstract

Process route planning bridges the gap between design stage and manufacturing stage, which transforms workblanks into parts or products. The decisions of processing methods, machines, cutting tools, and sequence of process stages during process route planning have a significant impact on carbon emissions in manufacturing process. To reduce carbon emissions of process routes of parts and simultaneously consider economic and high-efficiency factors, a low-carbon multi-objective process route optimization method is proposed. Firstly, a constructed PBOM (process bill of material) based on machining features of parts is used to quantify carbon emissions of every processing step. Secondly, a multi-objective optimization model of process routes with the objectives of minimum carbon emissions, minimum processing cost, and minimum processing time is built based on the PBOM. Thirdly, a multi-objective ant colony algorithm is designed to solve the proposed model. Finally, a practical applicable bearing seat is taken as a case study to verify the rationality of the proposed method. Comparison results show that the proposed method can obtain the low-carbon, economic, and high-efficiency process routes for parts.

Keywords Process route · Carbon emissions · Multi-objective optimization · Ant colony algorithm

1 Introduction

According to the research report of International Energy Agency [1], 1/3 of the energy consumption and 36% CO₂ emissions on the globe come from manufacturing industry. The statistical data from the energy statistics development of national bureau of statistics of China [2] also indicate that the

energy consumption of industrial circle accounts for about 71% of the total amount of energy consumption in China, and the manufacturing industry's energy consumption accounts for 81% of energy consumption in the whole industrial circle. Thus, low-carbon manufacturing [3] is emerged accordingly to solve the problem of high consumption, high emissions, and high pollution in manufacturing industry. Its ultimate goal is to reduce resource consumption and carbon emissions in the discrete manufacturing process including the stages of design [4], process planning, scheduling [5], and manufacturing [6].

Considering carbon emissions in process route planning plays an important role in realizing the low-carbon manufacturing. In machining process, process route planning bridges the gap between design stage and manufacturing stage, which transforms workblanks into parts or products. Especially in the process of intelligentized production nowadays, the process routes of different parts tend to have great flexibility, which means a part could be manufactured by different process routes. The flexibility of process route is reflected in the selection of process steps in the processing stages and sequencing of processing stages. In every processing stage, a manufacturing feature concerns the selection of processing methods, processing resources, and process tools

✉ Guang-hui Zhou
ghzhou@mail.xjtu.edu.cn

Chang-le Tian
tcl1992xajtdx@stu.xjtu.edu.cn

Jun-jie Zhang
zjjie16@stu.xjtu.edu.cn

Feng-tian Chang
ftchang@stu.xjtu.edu.cn

Qi Lu
luqi1234@stu.xjtu.edu.cn

¹ School of Mechanical Engineering, Xi'an Jiaotong University, Xi'an, Shannxi 710049, China

² State Key Laboratory of Manufacturing Systems Engineering, Xi'an Jiaotong University, Xi'an, Shannxi 710049, China

[7, 8], etc. In the sequencing of processing stages, the process steps selected in process stages are sequenced according to relevant restraints including precedence constraint among processing stages, and auxiliary time. The auxiliary time contains the machine change time, cutting tool change time, and clamp change time. The low-carbon process routes of parts are that the factors related to carbon emissions will be considered in the selection of processing steps and sequence decision of processing stages. Specifically, the factors are energy consumption of machines, usage of cutting fluid, changes of machine tools, changes of clamps, and abrasion of tools. Different processing methods, machines, sequences, cutting tools in process route planning cause large differences in carbon emissions generated by material, energy, and wastes. Hence, how to decide the optimal low-carbon process route according to the available manufacturing machines, methods, sequences, cutting tools, and so on is significant to reduce carbon emissions for manufacturing industries.

In fact, the optimization of process routes of parts has been widely researched by many scholars. This issue is integrated into different manufacturing systems, resources and environments, such as the integration of job scheduling and others [9–11]. However, these studies have the following limits: (1) Few scholars take carbon emissions as the objective of process route optimization of parts; (2) There are many complex and practical factors in quantifying carbon emissions during the manufacturing process. However, traditional carbon emissions quantitative models of process routes neglect many factors related to carbon emissions so that they are not sufficient and precise; (3) Many studies focus on single objective process route optimization. Processing time, cost, and quality are involved separately in their models rather than they are considered simultaneously. Hence, it has a great potential to study the process route optimization considering carbon emissions and other factors such as processing time and cost.

To address the above problems, this article proposes a process route optimization model considering carbon emissions factors to determine process routes, processing resources and relevant parameters during the whole manufacturing process in which the workblanks are turned into finished parts. The processing time and cost are also considered in the low-carbon process route optimization model. According to the research [12], a PBOM (process bill of material) model based on manufacturing features of parts is constructed firstly. On the basis of the PBOM, an assessment method is proposed to quantify carbon emissions of process routes of parts. Secondly, a process route optimization model considering carbon emissions, processing time, and cost is proposed. To solve this model, a multi-objective ant colony algorithm is introduced. In the end, a practical applicable case is applied to verify the feasibility and availability of the proposed model and algorithm. By comparison, the experimental results prove that the proposed method can not only reduce carbon

emissions and save cost and time but also obtain an optimal process route.

The rest of the paper is organized as follows. Section 2 reviews relevant research. Section 3 introduces carbon emissions quantitative model and Section 4 presents the optimization model based on the PBOM. Section 5 presents the solving process with the multi-objective ant colony algorithm. In Section 6, a case is tested to illustrate the implementation process and verify the feasibility and availability of the proposed method. Finally, conclusions are given in Section 7.

2 Literature review

Process route optimization problem plays an important role in manufacturing systems and it is studied by many scholars. Different methods are proposed to describe and optimize process routes to get near-optimal or optimal process routes with different constraints and goals. Process route optimization can be divided into two categories according to the number of considered objectives: one is the single objective optimization, which only pays attention to processing time or cost, and the other is the multi-objective optimization, which pays attention to time, cost, and other factors simultaneously.

In the traditional process route optimization, manufacturing cost or manufacturing time is widely considered as an important index. Lian et al. [13] considered different flexible factors in process route optimization and applied imperial competition algorithm to reduce comprehensive cost including processing cost, cutting tool cost, and machine cost. Liu et al. [14] considered processing cost, cutting tool change cost, and clamping cost and applied ant colony algorithm to solve the proposed process route optimization problem. Wen et al. [15] took three weighted sum of processing cost, cutting tool cost, and clamping cost as objective and solved the process route optimization model with honey-bee mating optimization (HBMO) algorithm. Li et al. [16] proposed a gene combined simulated annealing algorithm to solve the process route problem; the genetic algorithm was used to generate initial solution and the simulated annealing algorithm was applied to obtain optimal process routes. Qiao et al. [17] proposed a sequence method to sequence the selected process steps with genetic algorithm for box parts, and they took the weighted sum of constraints and objectives as the optimization fitness. Ma et al. [18] proposed a concurrent method to handle the process route optimization. On the other hand, many papers studied the process route optimization problem considering processing time from the integration of process planning and scheduling. Manupati et al. [19] proposed an integrated model based on non-cooperative game theory, and they solved it by a two-layer genetic algorithm and obtained the optimal completion time of each job. Shukla et al. [10] proposed a composite

algorithm based on combination of SA and TS and used agent technology to integrate process route and scheduling.

In the multi-objective process route optimization, Miljković et al. [20] took manufacturing time and manufacturing cost as optimization objectives, and they applied an improved particle swarm algorithm to solve the multi-objective process route optimization problem. Apart from time and cost, energy consumption and environmental factors have gradually been considered by many studies as optimization objectives in recent years. Srinivasan et al. [21, 22] studied the influences of processing sequence on environment based on features and explained the influences of features' processing sequence and the shape interference among features on environment. This is a great innovation on considering environmental factors. Newman et al. [23] proposed an oriented energy efficiency process planning theoretical framework. They found that both process routes and processing parameters will influence the energy consumption of machining process, and the energy consumption can be taken as the effective objective of process planning optimization. Tian et al. [24] proposed an energy consumption assessment method and a process planning optimization model for stochastic characteristics. Hu et al. [25] established an energy consumption optimization model based on processing sequence of features of parts. Altıntaş et al. [26] proposed an energy consumption prediction model for milling process of a cylindrical part. The model depended on the manufacturing features which came from STEP 224 application protocol that defined shape features and material characteristics of parts. Similarly, in some models [27, 28], according to the operation time of machine, energy consumption was divided into three different categories, i.e. energy consumption in the start-up phase, energy consumption in the operation phase and energy consumption in the material removal phase. However, owing to the great relationships between energy consumption and carbon emissions, few scholars consider the objective of carbon emissions. Wang et al. [29] integrated technology elements and proposed a combination model to assess carbon emissions in machining process. Yi et al. [30] established a process route optimization model aiming at the minimum carbon emissions and maximum processing efficiency. The model was optimized with NSGA-II, but in the process of optimization, the authors did not mention how to get the only solution which resulted in the failure of obtaining of the optimal leading edge. Meanwhile, the article did not consider the auxiliary carbon emissions between two adjacent process steps.

In conclusion, a review of the related work reveals that (1) one-dimensional objective such as processing time, or multi-dimensional objective by integrating and coupling many indicators is often taken as the decision objective in the traditional process route optimization research; (2) the energy consumption and carbon emissions are gradually considered with the introduction of low-carbon manufacturing. However, firstly,

the traditional process planning methods are hard to describe, represent, and solve the process planning problem restrained by carbon emissions. Secondly, low-carbon process route optimization has not been researched deeply, and most papers mainly focus on the energy consumption. Thirdly, low-carbon quantitative models of process routes neglect some factors such as auxiliary carbon emissions between two adjacent process steps. In view of the insufficiencies of current research on low-carbon process route optimization, this article develops a new method to precisely describe and effectively solve the process route optimization problem in process planning under the constraint of carbon emissions.

3 Carbon emission quantitative model of process route of parts

3.1 Calculation method of process step carbon emission based on PBOM

In the planning of process routes of parts, features are usually used to express and describe a part. A part is made up of one or several basic features. Basic features are divided into two categories, i.e., the auxiliary features and the main features. The main features, which includes faces, holes, chamfers, are those features that cannot be split again in geometric topology. The auxiliary features are local geometric structures of the main features including keyways, threads. For each standard shape machining feature, it needs a series of process states including rough machining, semi-finishing, and finish machining. Usually the selectable processing methods for a process state of a feature are not exclusive. Further, machines, cutting tools, and clamps for each process step are also selectable. Therefore, process route planning of parts devotes to select processing methods, processing resources, and so on in manufacturing process of features. Hence, a part usually has many selectable processing conditions so they correspond to different carbon emissions.

To quantify carbon emissions of process steps of process states of a part, a PBOM for specific parts is given. The structure of PBOM is shown in Table 1 and it includes the following four parts: the part structure information, operation information of basic features, process ID of process steps, and carbon emissions of each process step. The detailed explanation is as follows: (1) The part structure information has three levels, i.e., part level (P), composite feature (CF) and basic feature (BF); (2) Operation information of basic features is searched and filtered from the c-PBOM(carbon emissions-process bill of material) which is built for the manufacturing workshop [12]. Particularly, cutting parameters are added in this table, but they can be obtained by optimization finally; (3) Material carbon emissions generated by the production of raw materials, cutting tools, and cutting fluids consumed in a

Table 1 The structure of PBOM

Level, feature	Process elements						Process ID	Carbon emissions ($kgCO_2$)				
	Composite feature(CF)	Basic feature(BF)	Repeated information (R)	Method (M)	State (S)	Device (D)		Tool (T)	Clamp (C)	Cutting parameter	Material	Energy
Part(P)												
Sum												

machining process, energy carbon emissions caused by the production of the electricity consumed in a machining process, and waste carbon emissions, caused by the disposal of chips, scrap cutting tools, and scrap cutting fluids produced in a machining process are respectively obtained after the optimal cutting parameters are determined. The process ID includes the feature information and process elements, such as CF2F1R1S2M1D3T2C1. CF2F1 denotes the feature classification, R1 is repeated information and S2 is the second operation state. M1D3T2C1 represents that the used machine, process method, cutting tool and clamp are D3, M1, T2, and C1, respectively. The process ID is an important basis to decide carbon emissions from changes of cutting tools and clamps of parts features.

Process step is a continuous cutting process, and its life cycle includes the machine feeding, main shaft rotating, material removing, cutting fluid spraying, automatic chip removal, and basic module operation movement without tool changing movement. Therefore, the energy carbon emissions CE_{s-elec} within a process step are:

$$CE_{s-elec} = CE_{mr} + CE_{sp} + CE_f + CE_{bm} + CE_{cfs} + CE_{cc} \quad (1)$$

where CE_{mr} is carbon emissions from material removing, CE_{sp} is carbon emissions from the main drive, CE_f is carbon emissions from feeding, CE_{bm} is carbon emissions from basic module operation of machine, CE_{cfs} is energy carbon emissions from cutting fluid spraying, and CE_{cc} is carbon emissions from automatic chip removal.

The material carbon emissions $CE_{s-material}$ within a process step are:

$$CE_{s-material} = CE_{ptool} + CE_{pchip} + CE_{pcf} \quad (2)$$

where CE_{ptool} is carbon emissions from cutting tools production, CE_{pchip} is carbon emissions from workpiece material production, and CE_{pcf} is carbon emissions from cutting fluid production.

The waste carbon emissions $CE_{s-waste}$ within a process step are:

$$CE_{s-waste} = CE_{dtool} + CE_{dchip} + CE_{dcf} \quad (3)$$

where CE_{dtool} is carbon emissions from disposal of wasted cutting tools, CE_{dcf} is carbon emissions from the disposal of wasted cutting fluid, and CE_{dchip} is carbon emissions from the disposal of wasted cuttings chips.

The total carbon emissions within a process step are:

$$CE_{stage} = CE_{s-elec} + CE_{s-material} + CE_{s-waste} \quad (4)$$

All kinds of carbon emissions calculation models in the above formula are related to the process elements including workpiece materials, machines, cutting tools, cutting parameters. The specific carbon emissions models

can be acquired via literature [12] and Appendix (Tables 8, 9, 10, 11 and 12).

The machining process of a part involves the changes of possible automatic tools and clamps between two adjacent process steps, which also produces carbon emissions. Therefore, once the PBOM of parts is obtained, it is very easy to know the total carbon emissions of parts when auxiliary carbon emissions caused by auxiliary operation are provided.

3.2 Auxiliary carbon emission calculation method between process steps

Besides carbon emissions calculation of all process steps, the auxiliary carbon emissions calculation between two adjacent process steps are also needed. The auxiliary carbon emissions are from the changes of the possible automatic tools and clamps between process steps.

The auxiliary carbon emissions can be identified through the adjacent process numbers in process routes. Designing three rules in combination with the process numbers to reason carbon emissions between two adjacent process steps:

(1) Rule 1: Compare the numbered ID of machine between two adjacent process numbers from the given process route. If the values are different, it means that machine between the two process steps needs to be changed. The replacement of machines require the transportation process of parts between two machines. In this article, the transportation of the parts is treated as a process with a constant speed and constant power, and carbon emissions are determined by the length of the route of the transportation process. Therefore, carbon emissions CE_{transk} can be calculated as the following formula:

$$t_{transk} = (S_{(k-1)-k}) / v_{trans}$$

$$CE_{transk} = (P_{trans} + P_{bm}) \times t_{transk} \times EF_{elec} \tag{5}$$

where t_{transk} is the workpiece transportation time, $S_{(k-1)-k}$ is the distance between two machines, v_{trans} is the transportation speed of parts, P_{trans} is the transportation power, P_{bm} is the power of the basic module operation of machines, and EF_{elec} is carbon emission factor of electricity.

The replacement process of machines requires changes of the cutting tools and re-clamping operation of parts. Carbon emissions from changes of cutting tools and clamps can be calculated via rule 2 and rule 3.

(2) Rule 2: Based on Rule 1, compare the numbered ID of cutting tools between every two adjacent process numbers when the machines are identical. If the values are different, it means that the cutting tool required to change between the two adjacent process steps.

Carbon emissions of the automatic tool changes process CE_{tick} are constituted by carbon emissions generated by automatic tool changers and carbon emissions generated by the simultaneous operation of basic modules of machines. Therefore, CE_{tick} can be expressed as follows:

$$t_{tick} = n_t \times t_0$$

$$CE_{tick} = [(P_{tc} + P_{bm}) \times t_{tick} + E_{tcon} + E_{tcoff}] \times EF_{elec} \tag{6}$$

where n_t indicates the number of tool rotation of cutting change modules, t_0 is the time of each cutting tool change, P_{tc} is the power of cutting change module, E_{tcon} is the start energy consumption of cutting change module, E_{tcoff} is the shut off energy consumption of cutting change module, and EF_{elec} is carbon emissions factor of energy consumption.

(3) Rule 3: Compare the numbered ID of clamp between every two adjacent process numbers when machines are identical. If the values are different, it means that re-clamping is required.

The clamping process is usually completed by operation staff. Carbon emissions generated by the clamping process of machines can be calculated as follows.

$$CE_{clampk} = P_{bm} \times t_{clampk} \times EF_{elec} \tag{7}$$

where t_{clampk} in the formula depends on the time spent by the operation staff in clamp.

Therefore, the auxiliary carbon emissions between the two adjacent process steps are:

$$CE_{auxik} = CE_{transk} + CE_{tick} + CE_{clampk} \tag{8}$$

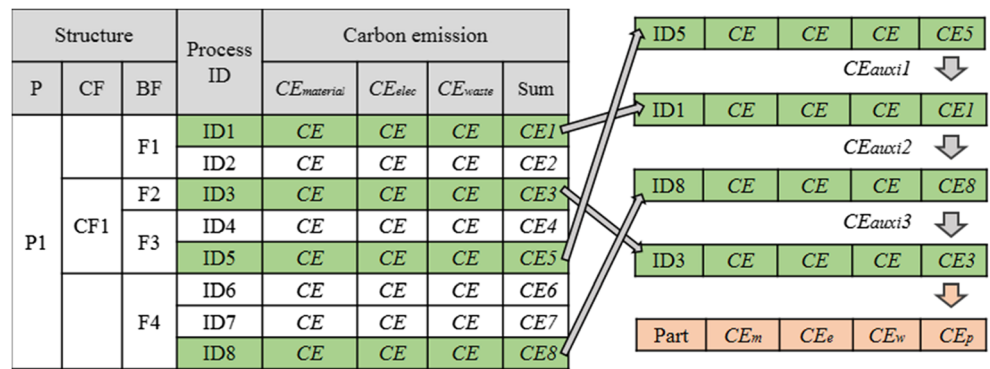
3.3 Carbon emissions of parts

Based on above discussion on calculation methods of carbon emissions of process steps and auxiliary carbon emissions between process steps, the processing step of every processing stage of all features of parts can be selected from the corresponding PBOM. Then the process steps selected in every processing stage are sequenced according to related constraints to form a process route of parts. Finally, carbon emissions of the process routes of parts can be obtained according to the calculation rules of auxiliary carbon emissions between process steps, shown in Eq. (9).

$$CE_{part} = \sum_{i=1}^n CE_{stage} + \sum_{k=1}^{n-1} CE_{auxik} \tag{9}$$

$$= \sum_{i=1}^n CE_{stage} + \sum_{k=1}^{n-1} CE_{transk} + \sum_{k=1}^{n-1} CE_{tick} + \sum_{k=1}^{n-1} CE_{clampk}$$

Fig. 1 Process route expression of a part using the PBOM



4 Process route optimization model based on PBOM

4.1 Expression of the process route of parts based on PBOM

The process route is the specific process procedure of parts, which includes processing sequence information between processing steps and processing steps themselves information. The manufacturing information includes machines, cutting tools, and cutting parameters. The processing sequence information is generally determined by many factors and constraints, such as machining accuracy, and processing experience. Moreover, different processing steps and processing sequences of the selected process steps will influence the auxiliary movement between process steps, which has an impact on the total carbon emissions of parts. In the meantime, the selected process steps and the movement between process steps also influence the total processing time and cost of parts. As a result, it is of great significance to consider the selection of process steps and the optimization of processing sequences.

4.1.1 Expression of process steps of parts based on PBOM

The PBOM contains all available manufacturing steps and resources of a part. A process route can be constructed based on the PBOM by selecting different process steps from all

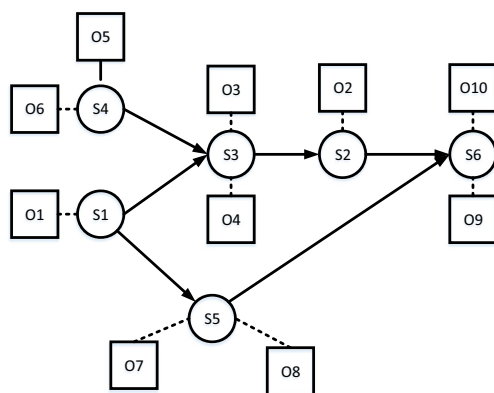


Fig. 2 Machining sequence constraint graph

processing stages of every feature. As such, different process routes have different carbon emissions, as shown in Fig. 1. For the feature F1 of the part P1, it has two alternative process steps, ID1 and ID2. Feature F3 also has two alternative process steps, ID4 and ID5. Similarly F4 has three alternative process steps, i.e., ID6, ID7, and ID8. Therefore, selecting process steps for each manufacturing feature constructs the process route of part P1. It is note that the selected process routes are not always rational because the constraints between manufacturing features are not considered in the machining process.

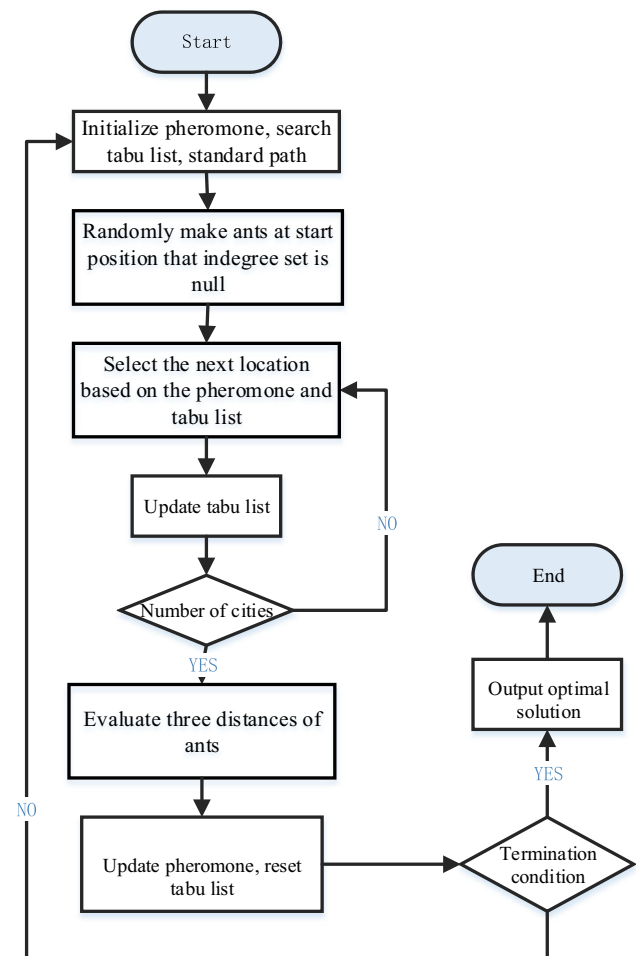
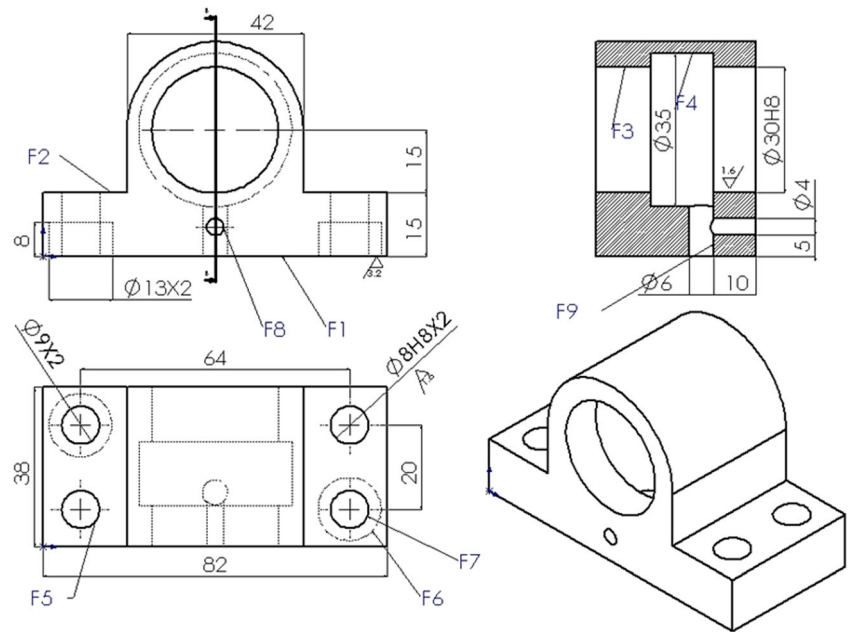


Fig. 3 Operation flow of multi-objective ant colony algorithm

Fig. 4 Three basic orthographic views of the bearing seat



4.1.2 Expression of processing sequence constraints

In the actual processing, these selected process steps from the PBOM cannot be arranged according to a random order. The arrangement of processing sequence of parts should follow the principles below based on considered factors which include the benchmark relationship of processing surfaces, the surfaces processing quality and the production efficiency.

- (1) Rough machining takes precedence over finish machining. It means that surface rough machining should be arranged before finish machining;
- (2) Primary surface priors to secondary surface. Primary surface is the principal factor in deciding the part quality, and its processing is also the main content in the whole technological processing. Therefore, the processing sequence should be considered to guarantee the machining precision of primary surface;
- (3) Plane machining takes precedence over hole machining. This means the plane (usually the assembly datum) should be processed firstly, and then the hole or hole series can be processed according to the plane datum. Normally, drilling a hole or boring a hole on semi-finished surfaces is likely to deflect the drill or split the tool.

These principles are all treated as the constraint conditions when arranging the process sequences. A constraint graph of processing stages can clearly indicate the sequence constraints among processing stages, because it is a visualized description of precedence relationship among process stages [31]. As

shown in Fig. 2, the symbol O_i indicates the alternative process steps for the processing stage S_j . The arrow represents the precedence relationship of process stages. It is noted that if the indegree set and outdegree set of one stage are both null, it reveals the stage has no any constraints with other stages; hence, it will not be shown in the constraint graph. Once the constraint graph is obtained, the selected alternative process steps of every processing stage could be combined and sorted in a reasonable process route. One of reasonable process routes shown in Fig. 2 is O1-O5-O7-O4-O2-O10.

4.2 Process route optimization model

From the above relationships of constraints, a great many reasonable process routes could be obtained. However, they might not be the optimal route when considering different objectives and constraints. The process route optimization is actually a combinational optimization problem with constraints. The mathematical model can be described in following section.

4.2.1 Optimization objective

Objective function: The optimization objective in this article is to minimize the processing time, carbon emissions and cost of parts, as shown in Eq. (10).

$$\min F(X) = \begin{cases} f_1(X) = T(X) = \sum t_{stage} + \sum t_{trans} + \sum t_{clampk} + \sum t_{tick} \\ f_2(X) = CE(X) = CE_{part} \\ f_3(X) = C(X) = \sum C_{stage} + \sum C_{auxik} \end{cases} \quad (10)$$

Table 2 The geometric structure of the bearing seat

Part	Composite feature	Basic feature	Replicate	Shape(mm)	Allowance
P1(bearing seat)		F1 (face)	1	82 × 38	3
		F2 (face)	2	20 × 38	2
	CF1 (bearing hole)	F3 (hole)	1	R15-r14	38
		F4 (hole)	1	R17.5-r15	15
		F5 (hole)	2	r4	15
	CF2 (counter bore)	F6 (hole)	2	r6.5	8
		F7 (hole)	2	r4.5	7
		F8 (hole)	1	r2	10
		F9 (hole)	1	r3	12.5

The processing time $T(X)$ of parts is the sum of cutting time of all process steps in process routes and all auxiliary time including machine change time, clamp change time, and cutting tools change time between two adjacent process steps. The cutting time of a process step can be expressed as Eq. (11):

$$t_{stage} = \begin{cases} l \times \Delta / f \times n \times a_p & \text{(turning, drill)} \\ V / f \times n \times a_p \times a_e & \text{(mill)} \end{cases} \quad (11)$$

where l is the feed distance, Δ is the machining allowance, V is the removing volume, a_p is the cutting depth, a_e is the cutting width, f is the feed rate, and n is the rotate speed.

The total amount of carbon emissions are the sum of the carbon emissions from process steps and the auxiliary carbon emissions between two adjacent process steps. Similarly, the processing cost also includes process steps cost C_{stage} and

auxiliary cost C_{aulik} between two adjacent process steps, which includes the processing management cost $[C_1 + C_2] \times T$, tool cost C_t , and cutting fluid cost C_{cf} . They can be calculated by the following Eq. (12):

$$\begin{aligned} C_{stage} &= [C_1 + C_2] \times T + C_t + C_{cf} \\ C_t &= \left[\frac{t_{cutting1}}{T_1 \times (R + 1)} + \dots + \frac{t_{cuttingi}}{T_i \times (R + 1)} + \dots \right] \times C_3 \\ C_{cf} &= \frac{t_{cutting}}{T_o} (M_o + AM_o) \times C_4 \\ C_{aulik} &= [C_1 + C_2] \times t_{aulik} \end{aligned} \quad (12)$$

where T_i is the times that the cutting tool would get sharpened, T_i is the cutting time using a specific cutting tool in a certain cutting condition, T_o is the cutting fluid change interval, T_i is the life cycle of the cutting tool in the certain cutting condition, AM_o is the initial volume in the

Table 3 The machine tools and cutting tools in the workshop

Machine tool	Cutting tool	Price(yuan)	Life cycle(min)
D1(CNC lathe)	T1 (Sandvik Boring tool CCMT 09T3 12-PR 4325)	30	75
D2(CNC horizontal miller)	T2(Sandvik Cemented carbide end mill D50)	50	42
	T3(Sandvik Cemented carbide end mill D20)	50	45
	T4(ZCCCT Cemented carbide end mill GM-2EL-D13)	111	60
	T5(ZCCCT SU series Cemented carbide twist drills $\phi 4$)	80	12
D3(Vertical driller)	T6(ZCCCT SU series Cemented carbide twist drills $\phi 6$)	80	25
D4(Radial driller)	T7(ZCCCT SU series Cemented carbide twist drills $\phi 8$)	80	25
	T8(ZCCCT SU series Cemented carbide twist drills $\phi 9$)	80	25
	T9(ZCCCT Cemented expanding drill $\phi 29$)	115	50
	T10(Cemented carbide reamer $\phi 8$)	120	45
	T11(Cemented carbide reamer $\phi 30$)	120	75
	T12(Countersink drill with parallel shanks and solid pilots $\phi 13$)	55	45

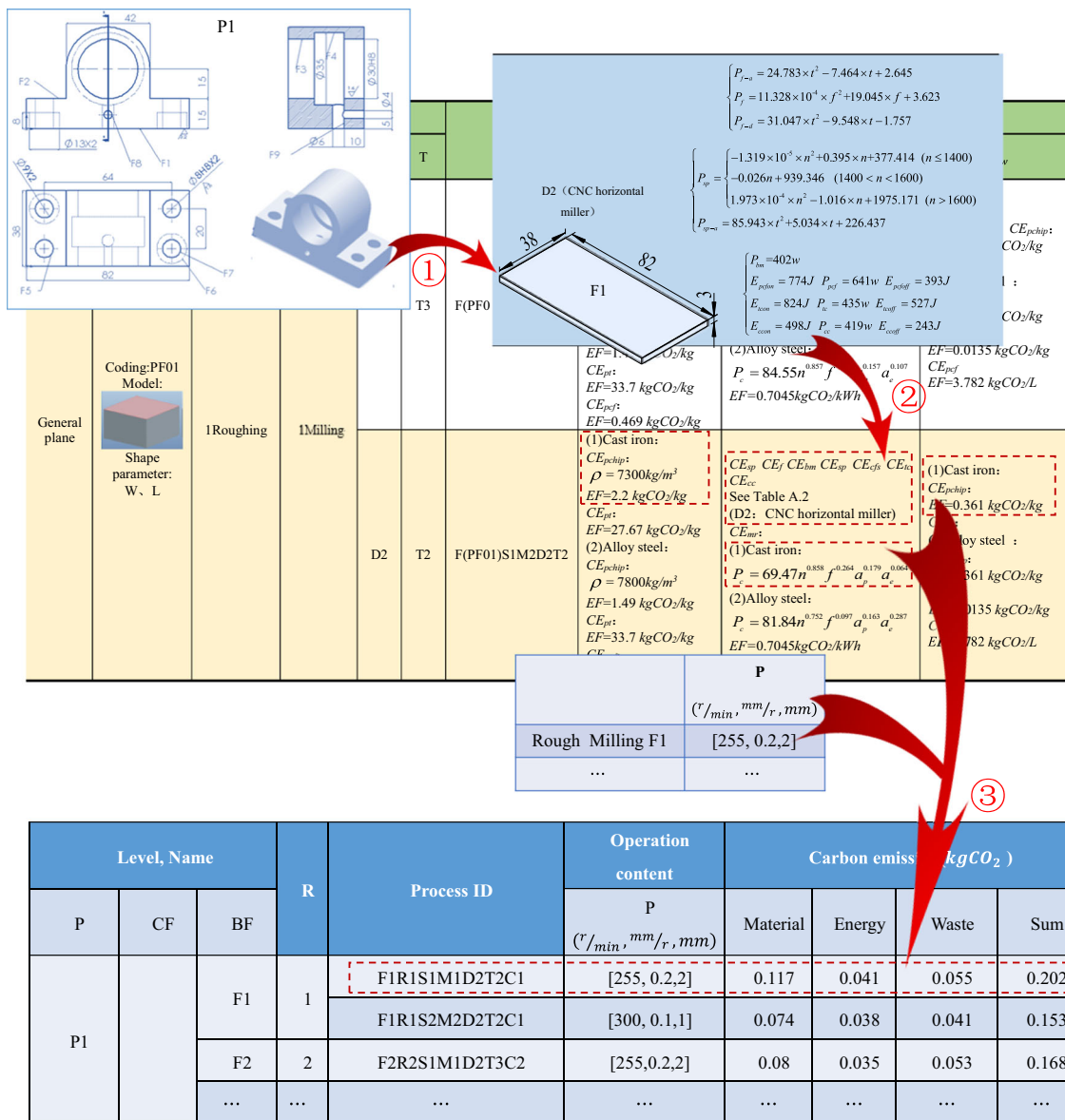


Fig. 5 The formation process of PBOM of the bearing seat

cutting fluid tank, M_o is the additional volume of cutting fluid during the life cycle, C_l is the depreciation cost for the equipment and management cost per unit time, C_2 is labor cost per unit time, C_3 is tool cost per unit time, and C_4 is cutting fluid cost per unit time.

4.2.2 Constraint conditions

There are many rationality constraints which have been discussed in machining process in Section 4.1.2. In the optimization model, these constraints are transformed into the constraint graph as the input conditions of the model.

5 Multi-objective ant colony optimization

5.1 Solving procedure

Ant Colony Algorithm is enlightened by the behavior that ants search for food. The behavior of real colonies foraging for food is simulated and used for solving optimization problems. The process route optimization problem is similar to the traveling salesman problem [32]. The nest of ants is deemed as the starting point of a city and food sources are regarded as target points. The whole path planning process is also considered as a process that the ants find food in the map city. Through mutual communication and coordination, ants eventually avoid obstacles and find an optimal path. The main operation

Table 4 The PBOM of the bearing seat

P	CF	BF	R	Operation content					Process ID			Carbon emission (kgCO ₂)			Sum
				S	M	D	T	C	P ($r'/\text{min}, r'/\text{min}, \text{mm}$)	Material	Energy	Waste			
P1	F1(face)	1	1 Rough	1 Milling	D2	T2	C1	[255,0,2,2]	F1R1S1M1D2T2C1	0.117	0.041	0.055	0.202		
			2 Finish	1 Milling	D2	T2	C1	[300,0,1,1]	F1R1S2M2D2T2C1	0.074	0.038	0.041	0.153		
	F2(face)	2	1 Rough	1 Milling	D2	T3	C2	[255,0,2,2]	F2R2S1M1D2T3C2	0.08	0.035	0.053	0.168		
			1 Rough	1 Counter boring	D3	T9	C3	[92,1,1,0,95]	CF1F3S1R1M1D3T9C3	0.095	0.073	0.078	0.246		
	CF1	1	1 Rough	1 Reaming	D4	T9	C3	[92,1,1,0,95]	CF1F3S1R1M1D4T9C3	0.095	0.062	0.078	0.235		
			2 Finish	1 Reaming	D3	T11	C3	[200,0,5,0,05]	CF1F3S2R1M1D3T11C3	0.026	0.049	0.034	0.109		
	F4(hole)	1	1 Rough	1 Boring	D1	T1	C3	[1120,0,4,2,5]	CF1F4S1R1M1D1T1C3	0.147	0.12	0.081	0.348		
			1 Rough	1 Drilling	D4	T7	C1	[500,0,36,3,95]	F5R2S1M1D4T7C1	0.128	0.103	0.095	0.326		
	CF2	2	1 Rough	1 Reaming	D4	T10	C1	[400,0,25,0,05]	F5R2S2M1D4T10C1	0.044	0.032	0.038	0.114		
			1 Rough	1 Counter sinking	D4	T12	C1	[630,1,6,5]	CF2F7R2S1M1D4T12C1	0.114	0.075	0.085	0.274		
P2	F7(hole)	2	1 Rough	1 Milling	D2	T4	C1	[255,1,6,5]	CF2F7R2S1M2D2T4C1	0.127	0.091	0.1	0.318		
			1 Rough	1 Drilling	D4	T8	C1	[630,1,4,5]	CF2F6R2S1M1D4T8C1	0.088	0.069	0.07	0.227		
	F8(hole)	1	1 Rough	1 Drilling	D3	T5	C3	[500,0,25,2]	F8R1S1M1D3T5C3	0.042	0.034	0.03	0.106		
			1 Rough	1 Drilling	D4	T5	C3	[500,0,25,2]	F8R1S1M1D4T5C3	0.042	0.033	0.03	0.105		
	F9(hole)	1	1 Rough	1 Drilling	D3	T6	C1	[500,0,36,3]	F9R1S1M1D3T6C1	0.055	0.048	0.051	0.154		
				D4	T6	C1	[500,0,36,3]	F9R1S1M1D4T6C1	0.055	0.045	0.051	0.151			

Table 5 Alternative step of each process state of the bearing seat

Features	Process state	step	Process ID	Processing time	Carbon emissions	cost
F1	S1	O1	F1R1S1M1D2T6C1	1.804	0.202	5.14
	S2	O2	F1R1S2M1D2T6C1	3.067	0.153	8.74
F2	S3	O3	F2R2S1M1D2T6C2	0.588	0.168	1.65
F3	S4	O4	CF1F3S1R1M1D3T9C3	0.474	0.246	1.33
		O5	CF1F3S1R1M1D4T9C3	0.474	0.235	1.33
	S5	O6	CF1F3S2R1M1D3T11C3	0.48	0.109	1.42
		O7	CF1F3S2R1M1D4T11C3	0.48	0.101	1.42
F4	S6	O8	CF1F4S1R1M1D1T4C3	0.056	0.348	0.15
F5	S7	O9	F5R2S1M1D4T7C1	0.122	0.326	0.41
	S8	O10	F5R2S2M1D4T10C1	0.22	0.114	0.71
F6	S9	O11	CF2F7R2S1M1D4T12C1	0.025	0.274	0.07
		O12	CF2F7R2S1M2D2T5C1	0.013	0.318	0.04
F7	S10	O13	CF2F6R2S1M1D4T8C1	0.032	0.227	0.11
F8	S11	O14	F8R1S1M1D3T5C3	0.136	0.106	0.57
		O15	F8R1S1M1D4T5C3	0.136	0.105	0.57
F9	S12	O16	F9R1S1M1D3T8C1	0.083	0.154	0.28
		O17	F9R1S1M1D4T8C1	0.083	0.151	0.28

steps of ant colony algorithm include the definition of distance between cities, probability choice of next city, and the update of the pheromone. Ant colony algorithm is successfully applied to solve a series of NP complete combinatorial optimization problems, such as quadratic assignment problems, and job shop scheduling problems. The flowchart of the algorithm is shown in Fig. 3.

5.2 The definition of distance between cities

The concept of distance between cities in ant colony algorithm is a criterion to judge the superiority of the ants passing paths. Processing time, processing cost, and carbon emissions of process steps are deemed as three distances from the last process step to the current process step. Each process step k_i corresponds to a city. The distances between process step k_i

and process step k_j are redefined as $time(k_i \rightarrow k_j)$, $carbon(k_i \rightarrow k_j)$, $cost(k_i \rightarrow k_j)$, as shown in eq. (13).

$$D = \begin{cases} distance_1 = time(k_i \rightarrow k_j) + time(k_j) \\ distance_2 = carbon(k_i \rightarrow k_j) + carbon(k_j) \\ distance_3 = cost(k_i \rightarrow k_j) + cost(k_j) \end{cases} \quad (i, j \in n) \tag{13}$$

where $time(k_i \rightarrow k_j)$ is the auxiliary time between city k_i and k_j , $carbon(k_i \rightarrow k_j)$ is auxiliary carbon emissions between city k_i and k_j , $cost(k_i \rightarrow k_j)$ is the cost from city k_i to k_j , and $time(k_j)$, $carbon(k_j)$, and $cost(k_j)$ are manufacturing time, carbon emissions, and cost of process step k_j respectively.

It is noted that the distances of ants to reach the first process step are the processing time, processing cost, and carbon emissions.

5.3 Tabu searching criterion

Ants must take the proper route when they crawl. In our algorithm, the next node that the ants crawl is the allowed node in the tabu list. They move according to the following rules:

- (1) Set T_i as tabu list of ant i . Ant i moves each step and stores this step and its corresponding processing stage in its own tabu list T_i .
- (2) According to the above constraint graph discussed in Section 4.1.2, in the rest nodes, the allowed nodes whose indegree set completely belongs to the tabu list or is null

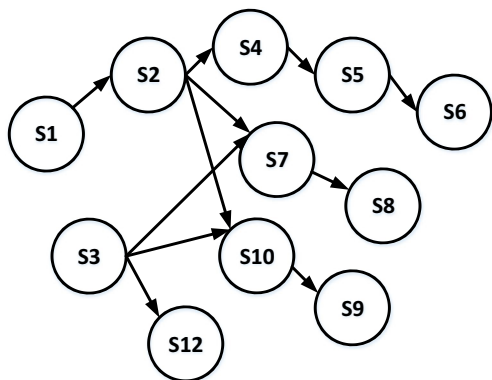


Fig. 6 The constraint graph of the process states of the bearing seat

Table 6 Parameter setting of the algorithm

Pheromone evaporation rate ρ	Pheromone weighting α	Heuristic information weight β	Minimum pheromone concentrations τ_{\min}	Reference Ant A_0
0.6	1	3	0.05	5

are obtained. Then one of these nodes is added to the tabu list T_i of ant i .

When all processing stages have a corresponding step to be added to the T_i , the ant i will complete an iteration, and its path is a process route.

$$P_{k_j k_{j+1}}^a(t) = \begin{cases} \frac{[\tau_{k_j k_{j+1}}(t)]^\alpha [\eta_{k_j k_{j+1}}(t)]^\beta}{\sum_{l \in M_{k_{j+1}}^a} [\tau_{k_j l}(t)]^\alpha [\eta_{k_j l}(t)]^\beta}, & k_{j+1} \in M_{k_j}^a \\ 0, & k_{j+1} \notin M_{k_j}^a \end{cases} \quad (14)$$

5.4 State transition probability

Each ant gradually chooses the next step from an initial step of parts to construct a process route. In each step of the route construction, step j of ant a moves from node k_j to the adjacent node k_{j+1} and the choice of k_{j+1} is carried out according to the state transition probability from node k_j to node k_{j+1} . The transition probability is designed as follows:

where $P_{k_j k_{j+1}}^a(t)$ denotes the probability of ant a from the current position k_j to the next position k_{j+1} at time t , $M_{k_{j+1}}^a$ is the optional set, namely the set of nodes that the ant can access in next step, which is obtained from the tabu list, $\tau_{k_i k_{j+1}}(t)$ is the pheromone concentration between k_j and k_{j+1} at time t , $\eta_{k_j k_{j+1}}(t)$ is local pheromone concentration at time t , generally obtained by the reciprocal of distance, and α and β are used to calculate the probability of transition.

Table 7 The optimal result of the bearing seat and a comparison with literature [12]

Literature [12]				This paper			
Process stage	Machine ID	Cutting tool ID	Clamp	Process stage	Machine ID	Cutting tool ID	Clamp
Rough milling F2	D2	T3	C2	Rough milling F1	D2	T2	C1
Rough milling F1	D2	T2	C1	Finish milling F1	D2	T2	C1
Finish milling F1	D2	T2	C1	Counter	D4	T9	C3
Counter boring F3	D3	T9	C3	Boring F3			
Reaming F3	D3	T11	C3	Reaming F3	D4	T11	C3
Boring	D1	T1	C3	Milling F2	D2	T3	C2
F4				Drilling F9	D4	T6	C1
Drilling	D4	T8	C1	Counter	D4	T12	C1
F6				Sinking F6			
Drilling	D4	T7	C1	Drilling F7	D4	T8	C1
F5				Drilling F5	D4	T7	C1
Reaming	D4	T10	C1	Reaming F5	D4	T10	C1
F5							
Drilling	D4	T6	C1	Boring F4	D1	T1	C3
F9				Drilling F8	D4	T5	C3
Countersinking F7	D4	T12	C1				
Drilling	D4	T5	C3				
F8							
CE = 2.451 kgCO ₂				CE = 2.43 kgCO ₂			
T = 19.636 min				T = 15.566 min			
C = 51.292 yuan				C = 37.786 yuan			

5.5 Pheromone trail updating

The key of the algorithm is to evaluate each path that ants crawl and determine the method of pheromone updating. Because the process route optimization in this paper is a multi-objective optimization problem, each path of the ant crawling has three targets, namely three distances indexes, which makes it difficult to measure the path. Many literatures used non-dominant relationship to find Pareto solution and determined the needed solution by normalization, which based on human experience. Based on the shortages of the traditional multi-objective solving approaches, this paper designs a novel pheromone trail updating mechanism based on the concept of ant colony algorithm.

Randomly assign an ant as a reference ant, and Q_i is the pheromone reference value of the ant under the action of objective i . In each iteration, the pheromone trail will be updated when all ants are constructed out their solution. The rule of pheromone trail updating pheromone release concentration $\Delta\tau_{k_j,k_{j+1}}(t)$ are as follows:

$$\begin{aligned} \tau_{k_j,k_{j+1}}(t+1) &= \max\left(\tau_{\min}, (1-\rho) \times \tau_{k_j,k_{j+1}}(t)\right. \\ &\quad \left. + \Delta\tau_{k_j,k_{j+1}}(t)\right) \\ \Delta\tau_{k_j,k_{j+1}}(t) &= Q_1/D_1(A_i) + Q_2/D_2(A_i) + \dots + [Q_n/D_n(A_i)]/n \end{aligned} \quad (15)$$

where $D_1(A_i)$ is the path distance from step k_j to k_{j+1} under the first objective of the ant A_i , n is the number of objectives, ρ is pheromone evaporation rate, $\tau_{k_j,k_{j+1}}(t)$ is pheromone between k_j and k_{j+1} at t time, and $\Delta\tau_{k_j,k_{j+1}}$ is the pheromone increment between k_j and k_{j+1} at t time. In this algorithm, the lower threshold of pheromone trace τ_{\min} is set up to avoid premature stagnation.

6 Case study

6.1 Features analysis of part

Taking a bearing, referred by [12], as an example to explain the feasibility and advantages of the proposed process route optimization method. Three basic orthographic views of the bearing seat are shown in Fig. 4 and the information of the geometric structure is listed in Table 2. The available machines and cutting tools in the workshop are listed in Table 3. The initial and additional dosages of cutting fluid are 500 and 200 L, the cutting fluid change interval is 2 months, and the times that the cutting tool would get sharpened is 3 at average. According to operation experiences, C_1 takes 2 yuan/min, C_2 takes 0.4 yuan/min, C_3 depends on the specific tools listed in Table 3, and C_4 takes 18.75 yuan/L. The average values are chosen as the

unit machine change time, unit machine change power, clamp change time, the basic module operation power, cutting tool change time, the cutting change module power and shut off-on energy consumption of cutting change module which are 40 s, 35 W, 1 min, 364.4 W, 1.2 s, 56.3 W, and 90 J, respectively [12].

According to the above PBOM formation steps shown in Section 3, the PBOM of feature F1 of this bearing can be obtained as shown in Fig. 5. The specific PBOM formation process of feature F1 is illustrated in Fig. 5. Firstly, the c-PBOM for the workshop is established; Secondly, according to the decomposed basic features F1 of the bearing seat, for example, the available operation elements and corresponding carbon emissions information are screened; Finally, filling in the obtained operation elements, carbon emissions information and the determined optimal cutting parameters into the corresponding fields of the PBOM until all the features of bearing seat are traversed. Table 4 gives the constructed PBOM of the bearing seat based on the research [12]. The solution space of the process route optimization of bearing seat is shown in Table 5, which is based on Eq. (12) and the PBOM of the bearing seat. In Table 5, there are many optional steps for each stage of each feature. For example, the processing stage S1 of the feature F3 has two steps: O3 and O4, and only one of them can be selected to add to the process routes.

Based on the processing sequence constraints of each processing stage of all features, the constraint graph of the process states of the bearing seat can be constructed as shown in Fig. 6.

6.2 Optimization result and discussion

According to the designed algorithm and optimal space of the bearing seat, we set the number of ants and the maximal iterations number as 20 and 200 respectively. Other parameters of the algorithm are listed in Table 6. The optimal process route of the bearing seat is calculated as listed in Table 7. The optimal processing time, cost, and carbon emissions are 37.786 yuan, 15.566 min and 2.43 kgCO₂ respectively.

We compare the process route, processing time, processing cost, and carbon emissions with literature [12]. The results are shown in Table 7. Through optimization, we can get that the cost reduced about 15 yuan, processing time reduced about 4.1 min, and carbon emissions decreased about 0.02 kg. It is observed that the proposed method could reduce carbon emissions, processing cost, and time obviously. Compared with the previous process route, we find that (1) the proposed method can save processing time, cost, and carbon emissions of process routes of parts without any changes of facilities in current

existing manufacturing environment; (2) the optimal solutions obtained by this optimization model can provide process routes with less changes of machines, cutting tools, and clamps under the constraints of processing time, cost, and carbon emissions. In the practical production, it plays a significant role in saving cost, improving delivery rate, and reducing carbon emissions.

7 Conclusion

In this paper, an approach of process route optimization is presented to reduce processing time, cost, and carbon emissions of parts. In current existing manufacturing environment, the approach can optimize carbon emissions, processing time, and cost of process route of parts without any changes of facilities. Several contributions are made from the proposed low-carbon, economic, and high-efficiency process route optimization method.

Firstly, the proposed quantified PBOM model can display the manufacturing resources and precisely calculate value of carbon emissions of each process step for parts.

Secondly, a multi-objective optimization model of process route with the objectives of minimum carbon emissions, minimum processing cost, and minimum cost is then built based

on the PBOM. The model can obtain a low-carbon, high-efficiency, and economic process routes by using the designed multi-objective ant colony algorithm.

Finally, the rationality and availability of the proposed method is verified by a bearing seat. Comparison results show that the proposed method can effectively reduce carbon emissions, processing time and cost of parts without any change of facilities. This will provide effective carbon emissions data of parts or products to cope with the coming carbon policy such as carbon labelling.

In manufacturing environment, job scheduling is another important module for parts manufacturing. Therefore, the process planning and scheduling are usually complementary. Thus, it is worth studying the integration method of route planning and scheduling to achieve the goal of global optimization of carbon emissions during the whole manufacturing process in the future.

Acknowledgments Special thanks are due to Ce Zhou for his gracious help of this work.

Funding information This research is supported by the National Natural Science Foundation of China (grant no. 51575435).

Appendix

Table 8 Partial machine tool power models of the workshop

Machine tool	Power models
D1(CNC lathe)	$\begin{cases} P_{f-a} = 106.656 \times t^2 - 5.853 \times t + 5.648 & P_f = -7.68 \times 10^{-4} \times f^2 + 22.614 \times f + 1.491 & P_{f-d} = 156.548 \times t^2 - 7.396 \times t - 2.513 \\ P_{sp} = \begin{cases} -5.944 \times 10^{-5} \times n^2 + 1.037 \times n - 182.139 & (n \leq 1100) \\ 0.145n + 716.650 & (1100 < n < 1500) \\ -1.21 \times 10^{-4} \times n^2 + 0.955 \times n - 255.443 & (n > 1500) \end{cases} & P_{sp-a} = 454.457 \times t^2 + 2.632 \times t - 265.966 \\ P_{bm} = 1679w & E_{pcon} = 294J & P_{pcf} = 418w & E_{pcfoff} = 92J & E_{tcon} = 398J & P_{tc} = 432w & E_{tcoff} = 214J \end{cases}$
D2(CNC horizontal miller)	$\begin{cases} P_{f-a} = 24.783 \times t^2 - 7.464 \times t + 2.645 & P_f = 11.328 \times 10^{-4} \times f^2 + 19.045 \times f + 3.623 & P_{f-d} = 31.047 \times t^2 - 9.548 \times t - 1.757 \\ P_{sp} = \begin{cases} -1.319 \times 10^{-5} \times n^2 + 0.395 \times n + 377.414 & (n \leq 1400) \\ -0.026n + 939.346 & (1400 < n < 1600) \\ 1.973 \times 10^{-4} \times n^2 - 1.016 \times n + 1975.171 & (n > 1600) \end{cases} & P_{sp-a} = 85.943 \times t^2 + 5.034 \times t + 226.437 \\ P_{bm} = 402w & E_{pcon} = 774J & P_{pcf} = 641w & E_{pcfoff} = 393J & E_{tcon} = 824J & P_{tc} = 435w & E_{tcoff} = 527J & E_{cccon} = 498J \\ P_{cc} = 419w & E_{cccoff} = 243J \end{cases}$
D3(Vertical driller)	$\begin{cases} P_{f-a} = 64.845 \times t^2 - 6.875 \times t + 3.429 & P_f = 5.299 \times 10^{-6} v_f^2 + 0.014 v_f - 1.224 & P_{f-d} = 46.689 \times t^2 - 11.925 \times t + 3.436 \\ P_{sp} = \begin{cases} 2.862 \times 10^{-5} \times n^2 + 1.042 \times n + 90.745 & (n \leq 1100) \\ 0.145n + 716.650 & (1100 < n < 1500) \\ 5.293 \times 10^{-4} \times n^2 - 0.955 \times n + 1274.985 & (n > 1500) \end{cases} & P_{sp-a} = 321.873 \times t^2 + 1.487 \times t + 26.849 \\ P_{bm} = 562w & E_{pcon} = 659J & P_{pcf} = 458w & E_{pcfoff} = 441J & E_{tcon} = 576J & P_{tc} = 480w & E_{tcoff} = 334J \end{cases}$
D4(Radial driller)	$\begin{cases} P_{f-a} = 135.714 \times t^2 - 9.857 \times t + 1.429 & P_f = 1.25 \times 10^{-4} \times f^2 - 0.055 \times f + 25 & P_{f-d} = 128.826 \times t^2 - 6.654 \times t + 2.844 \end{cases}$

Table 8 (continued)

Machine tool	Power models
Description	$\{ P_{sp} = \{ 1.944 \times 10^{-5} \times n^2 + 0.234 \times n + 422.750 \} (n < 1200) - 0.02 \times n + 751 \} (1200 < n < 1500) 2 \times 10^{-4} \times n^2 - 1.075 \times n + 1872.429 \} (n > 1500) P_{sp-a} = 354.457 \times t^2 + 2.632 \times t - 265.966$ $\{ P_{bm} = 466w E_{pcfon} = 355J P_{pcf} = 438w E_{pcfoff} = 208J E_{tcon} = 1864J P_{tc} = 795w E_{tcoff} = 634J$
	<p>P_{f-a}, P_f, P_{f-d}: Feed power in acceleration stage, uniform motion stage, and deceleration stage. P_{sp}, P_{sp}: Spindle rotation power in uniform motion stage and acceleration stage. P_{bm}: Power of basic modules (such as numerical control system, lighting, etc.). E_{pcfon}, E_{pcfoff}: Sudden energy consumption when the tool changer is turned on and turned off. P_{pcf}: Power of tool changer. E_{tcon}, E_{tcoff}: Sudden energy consumption when the cooling installation is turned on and turned off. P_{tc}: Power of cooling installation. E_{ccom}, E_{ccoff}: Sudden energy consumption when the automatic chip removing device is turned on and turned off. P_{cc}: Power of the automatic chip removing device.</p>

Table 9 Partial c-PBOM for rough machining of the workshop

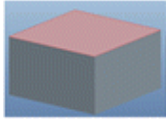
Feature	Operation element	ID
Name(F) General plane	Specification S M D T Coding:PF01 1Rough 1Milling D2 T2 Model: 	F(PF01)S1M1D2T2
Shape: W、L		
Description	ρ : Material density. EF: Carbon emission factor. $CE_{pchip}, CE_{pts}, CE_{pcf}$: Material carbon emissions of material production, cutting tool production and cutting fluid production. CE_{mr}, P_c : Carbon emissions of material removal and power of material removal. $CE_{dchip}, CE_{dtool}, CE_{def}$: Waste carbon emissions of chip disposal, cutting tool disposal, and cutting fluid disposal.	

Table 10 Partial c-PBOM for rough machining of the workshop (Continued)

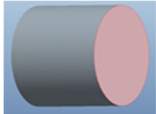
Feature		Operation element				ID	Carbon emission models			
Name(F)	Specification	S	M	D	T		$CE_{s,elec}$	$CE_{s,material}$	$CE_{s-waste}$	
End face	Coding: PF02 Model:	1Rough	1Turning	D1	T1	F(PF02)S1M1D1T1	(1)Cast iron: CE_{pchip} : $\rho = 7300 \text{ kg/m}^3$ $EF = 2.2 \text{ kgCO}_2/\text{kg}$ CE_{pt} : $EF = 12.9 \text{ kgCO}_2/\text{kg}$ (2)Alloy steel: CE_{pchip} : $\rho = 7800 \text{ kg/m}^3$ $EF = 1.49 \text{ kgCO}_2/\text{kg}$ CE_{pt} : $EF = 12.9 \text{ kgCO}_2/\text{kg}$ CE_{pcf} : $EF = 0.469$ kgCO_2/kg	$CE_{spr}, CE_f, CE_{bms}, CE_{spr}, CE_{cfs}, CE_{tc}, CE_{cc}$ See Table A.1 D1(CNC lathe) CE_{mr} : (1)Cast iron: $P_c = 53.74n^{0.953} f^{0.331} a_p^{0.791}$ (2)Alloy steel: $P_c = 57.23n^{0.861} f^{0.267} a_p^{0.787}$ $EF = 0.7045 \text{ kgCO}_2/\text{kWh}$	(1)Cast iron: CE_{pchip} : $EF = 0.361 \text{ kgCO}_2/\text{kg}$ CE_{pt} : $EF = 0.361 \text{ kgCO}_2/\text{kg}$ (2)Alloy steel: CE_{pchip} : $EF = 0.361 \text{ kgCO}_2/\text{kg}$ CE_{pt} : $EF = 0.135 \text{ kgCO}_2/\text{kg}$ CE_{pcf} : $EF = 3.782 \text{ kgCO}_2/L$	
										
	Shape parameter: D									
				2Milling	D2	T3	F(PF02)S1M2D2T3	(1) Cast iron: CE_{pchip} : $\rho = 7300 \text{ kg/m}^3$ $EF = 2.2 \text{ kgCO}_2/\text{kg}$ CE_{pt} : $EF = 11.4 \text{ kgCO}_2/\text{kg}$ (2) Alloy steel: CE_{pchip} : $\rho = 7800 \text{ kg/m}^3$ $EF = 1.49 \text{ kgCO}_2/\text{kg}$ CE_{pt} : $EF = 11.4 \text{ kgCO}_2/\text{kg}$ CE_{pcf} : $EF = 0.469$ kgCO_2/kg	$CE_{spr}, CE_f, CE_{bms}, CE_{spr}, CE_{cfs}, CE_{tc}, CE_{cc}$ See Table A.1 D2(CNC horizontal miller) CE_{mr} : (1) Cast iron: $P_c = 47.26n^{0.886} f^{0.42} a_p^{0.813}$ (2) Alloy steel: $P_c = 50.58n^{0.842} f^{0.146} a_p^{0.901}$ $EF = 0.7045 \text{ kgCO}_2/\text{kWh}$	(1) Cast iron: CE_{pchip} : $EF = 0.361 \text{ kgCO}_2/\text{kg}$ CE_{pt} : $EF = 0.361 \text{ kgCO}_2/\text{kg}$ (2) Alloy steel: CE_{pchip} : $EF = 0.361 \text{ kgCO}_2/\text{kg}$ CE_{pt} : $EF = 0.135 \text{ kgCO}_2/\text{kg}$ CE_{pcf} : $EF = 3.782 \text{ kgCO}_2/L$
				Description			ρ : Material density. EF : Carbon emission factor. $CE_{pchip}, CE_{pt}, CE_{pcf}$: Material carbon emissions of material production, cutting tool production, and cutting fluid production. CE_{mr}, P_c : Carbon emissions of material removal and power of material removal. $CE_{dchip}, CE_{dtool}, CE_{def}$: Waste carbon emissions of chip disposal, cutting tool disposal, and cutting fluid disposal.			

Table 11 Partial c-PBOM for rough machining of the workshop (Continued)

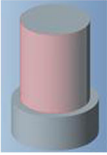


Feature	Specification	S	M	D	T	ID	Carbon emission models
Name (F) Cylindrical surface	1 Roughing CF02 Model: 	1	Turning	D1	T1	F(CF02)SIM1D1T1	$CE_{s-waste}$ (1) Cast iron: CE_{pchip} $EF = 0.361 \text{ kgCO}_2/\text{kg}$ CE_{pi} (2) Alloy steel: CE_{pchip} $EF = 0.361 \text{ kgCO}_2/\text{kg}$ CE_{pi} $EF = 0.0135 \text{ kgCO}_2/\text{kg}$ CE_{pcf} $EF = 3.782 \text{ kgCO}_2/\text{L}$
	Shape parameter: D, L						$CE_{s-material}$ $CE_{sp}, CE_j, CE_{bm}, CE_{sp}, CE_{cfs}, CE_{Lc}, CE_{Lcc}$ See Table A.1 D1(CNC lathe) CE_{mr} (1) Cast iron: $P_c = 63.74n^{1.035} f^{-0.154} a_p^{-0.807}$ (2) Alloy steel: $P_c = 67.23n^{0.991} f^{-0.218} a_p^{0.698} EF = 0.7045 \text{ kgCO}_2/\text{kWh}$
							CE_{s-elec} (1) Cast iron: CE_{pchip} $\rho = 7300 \text{ kg/m}^3$ $EF = 2.2 \text{ kgCO}_2/\text{kg}$ CE_{pi} $EF = 13.7 \text{ kgCO}_2/\text{kg}$ (2) Alloy steel: CE_{pchip} $\rho = 7800 \text{ kg/m}^3$ $EF = 1.49 \text{ kgCO}_2/\text{kg}$ CE_{pi} $EF = 13.7 \text{ kgCO}_2/\text{kg}$ CE_{pcf} $EF = 0.469 \text{ kgCO}_2/\text{kg}$
							$CE_{s-material}$ $CE_{sp}, CE_j, CE_{bm}, CE_{sp}, CE_{cfs}, CE_{Lc}, CE_{Lcc}$ See Table A.1 D1(CNC lathe) CE_{mr} (1) Cast iron: $P_c = 52.2n^{0.917} f^{0.203} a_p^{0.711}$ (2) Alloy steel: $P_c = 64.985V_c^{0.738} f^{0.434} a_p^{0.987} EF = 0.7045 \text{ kgCO}_2/\text{kWh}$
							CE_{s-elec} (1) Cast iron: CE_{pchip} $\rho = 7300 \text{ kg/m}^3$ $EF = 2.2 \text{ kgCO}_2/\text{kg}$ CE_{pi} $EF = 13.2 \text{ kgCO}_2/\text{kg}$ (2) Alloy steel: CE_{pchip} $\rho = 7800 \text{ kg/m}^3$ $EF = 1.49 \text{ kgCO}_2/\text{kg}$ CE_{pi} $EF = 13.2 \text{ kgCO}_2/\text{kg}$ CE_{pcf} $EF = 0.469 \text{ kgCO}_2/\text{kg}$
Description							ρ : Material density. EF : Carbon emission factor. CE_{pchip} , CE_{pi} , CE_{pcf} : Material carbon emissions of material production, cutting tool production, and cutting fluid production. CE_{mr} , P_c : Carbon emissions of material removal and power of material removal. CE_{dchip} , CE_{dtool} , CE_{dcf} : Waste carbon emissions of chip disposal, cutting tool disposal, and cutting fluid disposal.

Table 12 Partial c-PBOM for rough machining of the workshop (Continued)

Feature	Operation element	ID	Carbon emission models
Name (F) Cylindrical through hole	Specification S 1 Roughing 1 drilling D3 Coding: H01 Model:  Shape parameter: D, L	D T T7	$CE_{S-waste}$ (1) Cast iron: $CE_{E_{chip}}$ $EF = 0.361 \text{ kgCO}_2/\text{kg}$ $CE_{E_{pt}}$ (2) Alloy steel: $CE_{E_{chip}}$ $EF = 0.361 \text{ kgCO}_2/\text{kg}$ $CE_{E_{pt}}$ $EF = 0.0135 \text{ kgCO}_2/\text{kg}$ $CE_{E_{pcf}}$ $EF = 3.782 \text{ kgCO}_2/\text{L}$
			$CE_{S-material}$ $CE_{E_{sp}}, CE_{E_f}, CE_{E_{bm}}, CE_{E_{sp}}, CE_{E_{cf}}, CE_{E_{cc}}$ See Table A.1 D3(Vertical drilller) CE_{mr} (1) Cast iron: $P_c = 72.84D^{1.311} \rho^{0.237} v^{0.691}$ (2) Alloy steel: $P_c = 59.49D^{0.948} \rho^{0.457} v^{0.75}$ $EF = 0.7045 \text{ kgCO}_2/\text{kWh}$
Name (F) Cylindrical through hole	Specification S 1 Roughing 1 drilling D3 Coding: H01 Model:  Shape parameter: D, L	D T T8	$CE_{S-waste}$ (1) Cast iron: $CE_{E_{chip}}$ $EF = 0.361 \text{ kgCO}_2/\text{kg}$ $CE_{E_{pt}}$ (2) Alloy steel: $CE_{E_{chip}}$ $EF = 0.361 \text{ kgCO}_2/\text{kg}$ $CE_{E_{pt}}$ $EF = 0.0135 \text{ kgCO}_2/\text{kg}$ $CE_{E_{pcf}}$ $EF = 3.782 \text{ kgCO}_2/\text{L}$
			$CE_{S-material}$ $CE_{E_{sp}}, CE_{E_f}, CE_{E_{bm}}, CE_{E_{sp}}, CE_{E_{cf}}, CE_{E_{cc}}$ See Table A.1 D3(Vertical drilller) CE_{mr} (1) Cast iron: $P_c = 57.26D^{1.294} \rho^{0.198} v^{0.716}$ (2) Alloy steel: $P_c = 46.49D^{1.013} \rho^{0.325} v^{0.547}$ $EF = 0.7045 \text{ kgCO}_2/\text{kWh}$

ρ : Material density.
 EF : Carbon emission factor.
 $CE_{E_{chip}}, CE_{E_{pt}}, CE_{E_{pcf}}$: Material carbon emissions of material production, cutting tool production and cutting fluid production.
 CE_{mr}, P_c : Carbon emissions of material removal and power of material removal.
 $CE_{E_{chip}}, CE_{E_{tool}}, CE_{E_{def}}$: Waste carbon emissions of chip disposal, cutting tool disposal, and cutting fluid disposal.

References

- IEA (2009) World energy outlook 2008. OECD
- Liu Z (2015) China's carbon emissions report 2015. Harvard Kennedy School, Cambridge
- Tridech S, Cheng K (2011) Low carbon manufacturing: characterization, theoretical models and implementation. *Int J Manuf Res* 6(6):110–121. <https://doi.org/10.1504/IJMR.2011.040006>
- Tao F, Bi LN, Zuo Y, Nee AYC (2016) A hybrid group leader algorithm for green material selection with energy consideration in product design. *CIRP Ann Manuf Technol* 65(1):9–12. <https://doi.org/10.1016/j.cirp.2016.04.086>
- Zhang YF, Wang J, Liu Y (2017) Game theory based real-time multi-objective flexible job shop scheduling considering environmental impact. *J Clean Prod* 167:665–679
- Zhang YF, Ren S, Liu Y, Si S (2017) A big data analytics architecture for cleaner manufacturing and maintenance processes of complex products. *J Clean Prod* 142(Part 2):626–641
- Bo ZW, Hua LZ, Yu ZG (2006) Optimization of process route by genetic algorithms. *Robot Cim Int Manuf* 22(2):180–188. <https://doi.org/10.1016/j.rcim.2005.04.001>
- Wang W, Li Y, Huang L (2016) Rule and branch-and-bound algorithm based sequencing of machining features for process planning of complex parts. *J Intell Manuf*: 1–8
- Hua GR, Zhou XH, Ruan XY (2007) GA-based synthesis approach for machining scheme selection and operation sequencing optimization for prismatic parts. *Int J Adv Manuf Technol* 33(5–6):594–603. <https://doi.org/10.1007/s00170-006-0477-7>
- Shukla SK, Tiwari MK, Son YJ (2008) Bidding-based multi-agent system for integrated process planning and scheduling: a data-mining and hybrid tabu-SA algorithm-oriented approach. *Int J Adv Manuf Technol* 38(1–2):163–175. <https://doi.org/10.1007/s00170-007-1087-8>
- Zhou GH, Xiao ZD, Jiang PY, Huang GQ (2010) A game-theoretic approach to generating optimal process plans of multiple jobs in networked manufacturing. *Int J Comput Integr Manuf* 23(12):1118–1132. <https://doi.org/10.1080/0951192X.2010.524248>
- Zhou GH, Zhou C, Tian CL and Xiao ZD (2017) Feature-based carbon emission quantitation strategy for the part machining process. *Int J Comput Integr Manuf*: 1–20
- Lian K, Zhang C, Shao X, Gao L (2012) Optimization of process planning with various flexibilities using an imperialist competitive algorithm. *Int J Adv Manuf Technol* 59(5–8):815–828. <https://doi.org/10.1007/s00170-011-3527-8>
- Liu XJ, Yi H, Ni ZH (2013) Application of ant colony optimization algorithm in process planning optimization. *J Intell Manuf* 24(1):1–13
- Wen XY, Li XY, Gao L, Sang HY (2014) Honey bees mating optimization algorithm for process planning problem. *J Intell Manuf* 25(3):459–472. <https://doi.org/10.1007/s10845-012-0696-8>
- Li WD, Ong SK, Nee AYC (2002) Hybrid genetic algorithm and simulated annealing approach for the optimization of process plans for prismatic parts. *Int J Prod Res* 40(8):1899–1922. <https://doi.org/10.1080/00207540110119991>
- Qiao L, Wang XY, Wang SC (2000) A GA-based approach to machining operation sequencing for prismatic parts. *Int J Prod Res* 38(14):3283–3303. <https://doi.org/10.1080/002075400418261>
- Ma ZQ, Zhang P, Gu M, Sun L, Sun XL, Cheng Q, Wei J (2014) Process route optimization for machining center NC milling manufacturing. *Appl Mech Mater* 455:561–567
- Manupati VK, Deo S, Cheikhrouhou N, Tiwari MK (2012) Optimal process plan selection in networked based manufacturing using game-theoretic approach. *Int J Prod Res* 50(18):5239–5258. <https://doi.org/10.1080/00207543.2012.682181>
- Miljković Z, Petrović M (2017) Application of modified multi-objective particle swarm optimisation algorithm for flexible process planning problem. *Int J Comput Integr Manuf* 30:1–21
- Srinivasan M, Sheng P (1999) Feature-based process planning for environmentally conscious machining—part 1: microplanning. *Robot Comput Integr Manuf* 15(15):257–270. [https://doi.org/10.1016/S0736-5845\(99\)00017-4](https://doi.org/10.1016/S0736-5845(99)00017-4)
- Srinivasan M, Sheng P (1999) Feature based process planning in environmentally conscious machining—part 2: macroplanning. *Robot Comput Integr Manuf* 15(3):271–281. [https://doi.org/10.1016/S0736-5845\(99\)00018-6](https://doi.org/10.1016/S0736-5845(99)00018-6)
- Newman ST, Nassehi A, Asrai RI, Dhokia V (2012) Energy efficient process planning for CNC machining. *CIRP Ann Manuf Technol* 5(2):127–136. <https://doi.org/10.1016/j.cirp.2012.03.007>
- Tian G, Liu Y, Ke H, Chu J (2012) Energy evaluation method and its optimization models for process planning with stochastic characteristics: a case study in disassembly decision-making. *Comput Ind Eng* 63(3):553–563. <https://doi.org/10.1016/j.cie.2011.08.011>
- Hu L, Peng C, Evans S, Peng T, Liu Y, Tang R, Tiwari A (2017) Minimising the machining energy consumption of a machine tool by sequencing the features of a part. *Energy* 121:292–305. <https://doi.org/10.1016/j.energy.2017.01.039>
- Altıntaş RS, Kahya M, Ünver HÖ (2016) Modelling and optimization of energy consumption for feature based milling. *Int J Adv Manuf Technol* 86(9–12):3345–3363
- Balogun VA, Mativenga PT (2013) Modelling of direct energy requirements in mechanical machining processes. *J Clean Prod* 41(2):179–186. <https://doi.org/10.1016/j.jclepro.2012.10.015>
- Yin R, Cao H, Li H, Sutherland JW (2014) A process planning method for reduced carbon emissions. *Int J Comput Integr Manuf* 27(12):1175–1186. <https://doi.org/10.1080/0951192X.2013.874585>
- Wang Y, Zhang H, Zhang Z, Wang J (2015) Development of an evaluating method for carbon emissions of manufacturing process plans. *Discrete Dyn Nat Soc*:1–8
- Yi Q, Li C, Zhang X, Liu F, Tang Y (2015) An optimization model of machining process route for low carbon manufacturing. *Int J Adv Manuf Technol* 80(5–8):1181–1196
- Wang J, Wu X, Fan X (2015) A two-stage ant colony optimization approach based on a directed graph for process planning. *Int J Adv Manuf Technol* 80(5–8):839–850. <https://doi.org/10.1007/s00170-015-7065-7>
- Dorigo M, Gambardella LM (1997) Ant colony system: a cooperative learning approach to the traveling salesman problem. *IEEE Trans Evol Comput* 1(1):53–66. <https://doi.org/10.1109/4235.585892>